Universiteit van Amsterdam
Institute for Interdisciplinary Studies

MSc Complex Systems and Policy
Model-Based Decision Making
Assignment 3

Transition to Electric Vehicles: Adoption, Coordination & Policy Intervention

Submitted by:

Simona Lupșa	16421604
Eva Wehrle	16433718

December 15, 2025

1. Introduction & Policy Relevance

The transition to electric vehicles (EVs) is a key part of Europe's strategy to reduce its carbon emissions. In 2022, the transport sector accounted for almost a quarter of EU greenhouse gas emissions, with road transport being the main source (European Environment Agency, 2024). Therefore, achieving the EU Green Deal's goal of climate neutrality by 2050 and the interim target of reducing emissions by 55% by 2030 (relative to 1990) requires a rapid shift towards electric mobility from internal combustion engine vehicles (European Commission, no date). In line with the Paris Agreement, this transition delivers important additional benefits, including improved urban air quality, reduced energy dependence and support for the deployment of renewable electricity (European Environment Agency, 2024).

However, the EV transition presents the typical coordination challenge of systems with network externalities. Adoption depends not only on individual preferences, but also on the availability of complementary infrastructure, particularly charging stations. In the early stages of diffusion, potential adopters face a 'Stag Hunt'-type dilemma: although collective adoption yields higher payoffs through better infrastructure and interoperability, early adopters may fare worse in environments with limited infrastructure. This can result in persistent low-adoption equilibria, underinvestment, and path dependence, increasing the risk of lock-in to fossil-based mobility systems (Arthur, 1989; Shove, 2012). Once a critical adoption threshold is reached, positive feedback loops between EV uptake and charging infrastructure can generate self-reinforcing diffusion towards electrification.

This report employs a networked agent-based model that represents EV diffusion as a Stag Hunt coordination game. The following sections explore baseline dynamics, network effects, and potential policy interventions.

2. Methods and Experimental Design

The analysis follows a three-part experimental approach using a networked agent-based model implemented in Mesa and NetworkX. Agents occupy nodes in a network, representing individual drivers choosing between adopting an electric vehicle (C) or remaining with a conventional car (D). Their payoffs follow a Stag Hunt coordination game, where the utility from mutual adoption depends on a global infrastructure variable $I(t)$. Infrastructure evolves based on aggregate EV adoption, creating a positive feedback loop between adoption and infrastructure availability:

$$a(I) = a_0 + \beta_I I(t), I(t+1) = I(t) + g_I(X(t) - I(t))$$

2.1 Baseline System Analysis

The first set of experiments investigates the model's intrinsic dynamics in the absence of policy interventions. Parameter sweeps across initial adoption levels X_0, initial infrastructure I_0, and infrastructure feedback strength β_I reveal how endogenous tipping phenomena emerge. For visualization we use heatmaps of final EV adoption as a function of (X_0, I_0) and $(X_0, \frac{a(I)}{b})$, phase plots of system trajectories $(I(t), X(t))$ and sensitivity analyses for different β_I. These experiments identify bistability regions and thresholds that mark transitions between low- and high-adoption equilibria, providing a diagnostic baseline for later interventions.

All simulations are conducted on networks of $N = 400$ agents, to balance computational feasibility and the showcase of structural characteristics. As such, the networks are sufficiently large to exhibit meaningful clustering and structural heterogeneity, while remaining small enough to permit broad

parameter sweeps and repeated stochastic simulations that yield robust average outcomes. Moreover, each simulation is run for $T = 50$ time steps. Preliminary trial runs with longer horizons ($T = 200$ and $T = 100$) showed that the model consistently converges much earlier, indicating that a horizon of 50 steps is sufficient to capture the full transition dynamics and final equilibrium behaviour, thereby providing a clear picture of the system's outcomes. Baseline model parameters are held fixed across all experiments and are varied only when explicitly swept to study their isolated effects.

The (X_0, I_0) heatmaps explore both parameters over the full unit interval $[0, 1]$, discretized into evenly spaced grids. This range captures all plausible initial conditions, from near-zero adoption and infrastructure to fully saturated states. Using the full domain allows clear identification of critical boundaries separating basins of attraction. Similarly, the payoff ratio $\frac{a(I)}{b}$ is swept to span regimes below, within, and above the tipping region, with the same purpose of providing a clear visualization of how coordination incentives reshape equilibrium structure and adoption levels. Finally, the infrastructure feedback strength β_I is varied in a dedicated sensitivity analysis to assess how strongly infrastructure responsiveness amplifies or dampens adoption dynamics.

It is important to note that all heatmap experiments are conducted on two network structures: Erdős–Rényi (ER) random networks and Barabási–Albert (BA) scale-free networks. Although this adds to the computational costs of the experiment, it serves as an opportunity to observe which features of the diffusion process are intrinsic to the coordination model itself, and which are amplified or suppressed by specific network structures. This distinction is meant to help in assessing the influence of specific parameters, remaining to discuss how network topology affects diffusion in later experiments.

Each parameter combination is evaluated using 20 stochastic realizations, and outcomes are averaged to reduce noise arising from random initialization and network generation. This aggregation emphasizes robust structural effects rather than idiosyncratic outcomes of individual runs.

2.2 Network Structure Analysis

The second part examines how adoption dynamics depend on network topology. Simulations are conducted on different graph structures each capturing different patterns of local connectivity and information diffusion. In addition to the BA an ER network mentions above we used Watts–Strogatz (WS) small-world networks. To evaluate the impact of network topology, we measure adoption speed, probability of reaching high-adoption equilibria, cluster formation, as well as network-specific sensitivity to tipping.

A regular grid network is intentionally excluded from the analysis. While grid structures are analytically convenient, they impose highly constrained and spatially uniform connectivity patterns that are not representative of real-world scenarios. In contrast, the selected network classes allow for heterogeneous degrees, shortcut connections, and varying levels of clustering, all of which are known to play a role in diffusion and coordination processes.

Each network topology is chosen to isolate specific structural mechanisms relevant to coordination dynamics. ER networks have minimal clustering, while WS networks introduce high clustering combined with short average path lengths, enabling the study of how local reinforcement and shortcuts jointly affect adoption cascades. Additionally, BA networks capture degree heterogeneity and hub dominance, making it possible to assess how influential agents and unequal connectivity influence tipping behaviour. All networks are constructed with similar mean degree to ensure that differences in diffusion outcomes are primarily driven by topological structure. By comparing these network classes

under identical parameters, the experiments isolate topology-dependent effects and clarify how different structural features shape coordination, resilience, and diffusion speed.

For each network structure, simulations are conducted over a range of initial adoption levels and seeding strategies (random seeding and highest-degree seeding), generating time series of adoption that are subsequently analysed using multiple complementary metrics. The experimental design relies on a single comprehensive simulation run per network, from which all outcome measures are derived, ensuring consistency across analyses.

From the resulting trajectories, we assess adoption speed through mean time-evolution curves, equilibrium behaviour through final adoption distributions and the probability of reaching a high-adoption equilibrium, and structural diffusion patterns through the dispersion and clustering of trajectories over time. Multiple stochastic realizations are performed for each parameter setting and aggregated to reduce noise from random initialization and network generation, allowing observed differences in outcomes to be attributed to network structure rather than idiosyncratic fluctuations.

2.3 Policy Intervention

Building on the mechanisms identified in the network and adoption analyses, we evaluate a targeted policy intervention aimed at overcoming early coordination failures. The conceptual motivation and policy interpretation of the intervention are introduced in Section 4.

Methodologically, the intervention is implemented as a parametric modification of initial conditions and adoption incentives. Relative to the no-intervention baseline, the intervention increases the initial adoption share by an additional fraction Δa through targeted seeding of high-degree nodes. In selected simulations, adoption incentives are further adjusted by temporarily modifying payoff parameters (a_0, b) over a fixed intervention window T. Intervention intensity (Δa), timing, and duration are varied systematically across simulations and evaluated under ER, WS, and BA network topologies. All other model parameters are held constant to ensure that observed differences in outcomes are attributable to the intervention rather than baseline dynamics.

3. Results

3.1 Baseline System Analysis

For the random (ER) network, baseline dynamics are largely governed by the initial adoption level X_0, while infrastructure $I(t)$ responds only weakly over the simulated time horizon (Figure 1). When X_0 is low, trajectories in the (X, I) phase plane display slow and irregular motion, remaining near low adoption levels without converging to a clear stable fixed point. In some cases, adoption drifts back toward lower values, indicating fragile low-adoption dynamics rather than a well-defined equilibrium. As X_0 increases, trajectories move rapidly toward high adoption levels and approach near-full adoption ($X(t) \approx 1$), while remaining almost horizontal. This pattern indicates that adoption dynamics operate on a much faster timescale than infrastructure adjustments, implying dominance of imitation dynamics with only limited infrastructure feedback. Although some path dependence is present, sufficiently high initial adoption can tip the system toward sustained high adoption. However, the absence of a robust low-adoption attractor, together with minimal changes in $I(t)$, suggests weak or incipient bistability rather than two clearly separated stable equilibria.

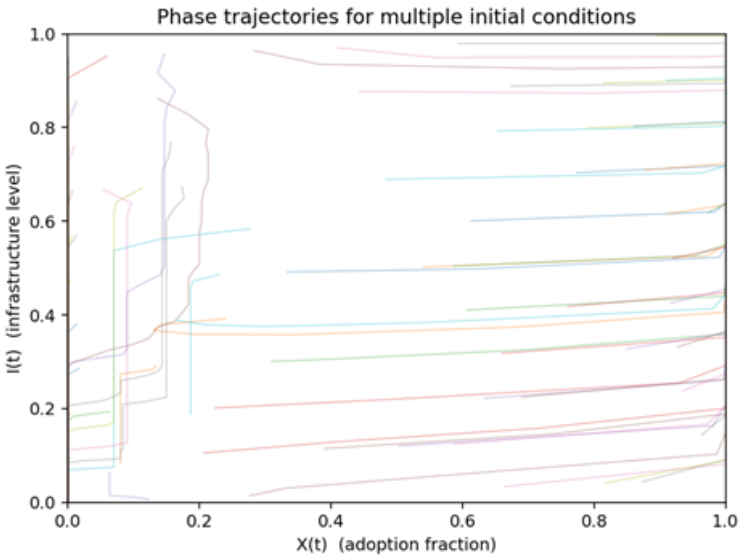

Figure 1: Phase trajectories for different initial conditions in (X, I)-space, where the x-axis represents the level of EV adoption and the y-axis represents the infrastructure level.

The heatmap of final adoption outcomes as a function of initial adoption $X_0$and initial infrastructure I_0 for the ER network (Figure 2, left) shows a sharp, nearly vertical threshold at $X_0 \approx 0.35$. Above this threshold, the system almost always converges to full adoption, whereas below it adoption collapses regardless of the initial infrastructure level. The near-vertical transition indicates that I_0 has little influence on long-run outcomes. The same pattern is observed for the scale-free network; however, the transition is less sharp in the scale-free network (Figure 2, right), This is suggesting that final adoption is primarily determined by X_0rather than network topology. However, the transition is less sharp in the scale-free network.

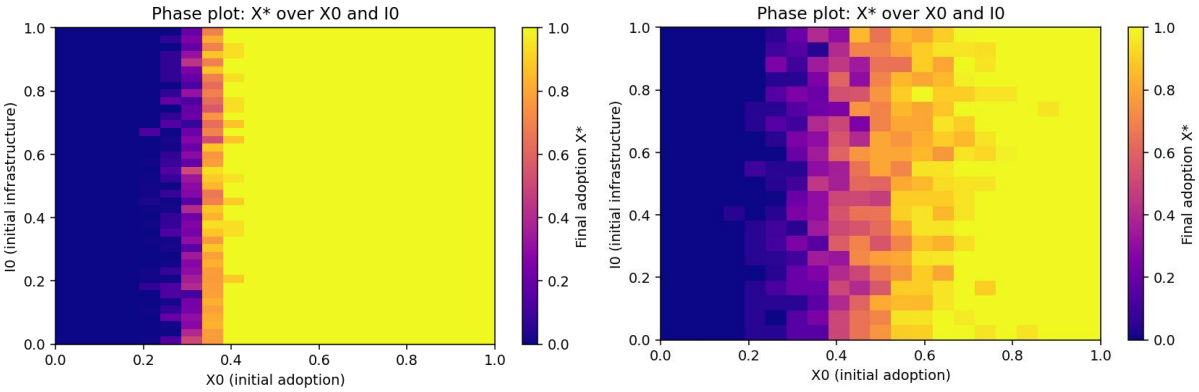

Figure 2: 1-D heat maps of the final adoption rate as a function of initial adoption (x-axis) and initial infrastructure (y-axis) for the random (ER) network (left panel) and the scale-free (BA) network (right panel).

Figure 3 presents final adoption X^*as a function of X_0 and the payoff ratio a_I/b. For the ER network, a clear tipping boundary separates low- and high-adoption regimes. Low payoff ratios lead to declining adoption even at moderate X_0, whereas higher ratios expand the region of full adoption, allowing small initial seeds to trigger large cascades. This behavior is consistent with coordination-game bistability. The scale-free network exhibits the same qualitative dependence on X_0 and a_I/b, but the transition is less sharp, with broader regions of partial adoption. A possible explanation is that random seeding does not systematically activate high-degree hubs, which may face higher effective adoption thresholds and impede cascades. Conversely, when hubs are seeded, widespread adoption can occur. As targeted seeding was not explored, this interpretation remains speculative. Overall, degree heterogeneity appears to reduce the clarity of convergence and increase mixed-adoption outcomes.

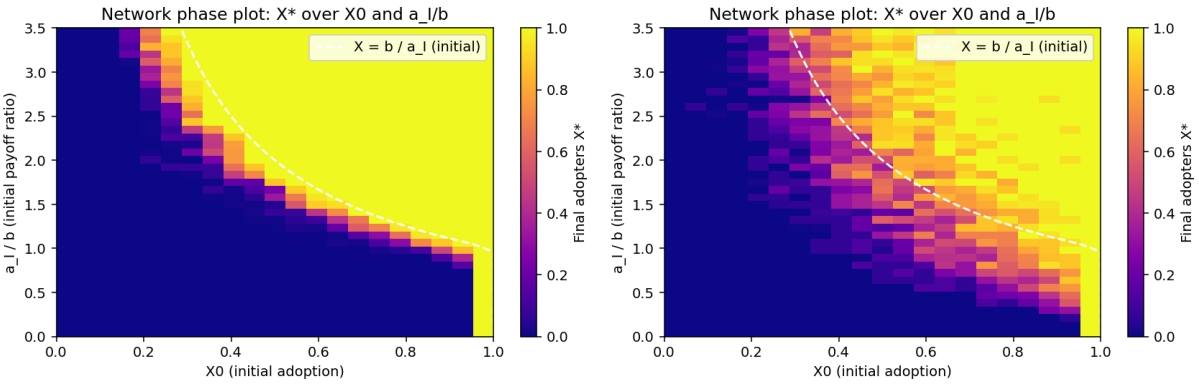

Figure 3: Network phase plots of final adoption X^*as a function of initial adoption X_0(x-axis) and the payoff ratio a_I/b(y-axis) for the ER network (left panel) and the scale-free network (right panel).

Finally, sensitivity analysis of the infrastructure feedback strength $\beta_I$reveals highly non-monotonic effects on final adoption X^*(Figure 4). Adoption fluctuates strongly across values of β_I, with pronounced minima at $\beta_I \approx 0, 0.5, 1,$ and 3, and a single maximum around $\beta_I \approx 2$–2.5. Since $\beta_I$affects only the slow-moving infrastructure dynamics, its influence on adoption payoffs remains limited. Overall, the results suggest that varying β_I alone does not provide a robust mechanism for sustaining adoption and does not eliminate the system's sensitivity to initial conditions.

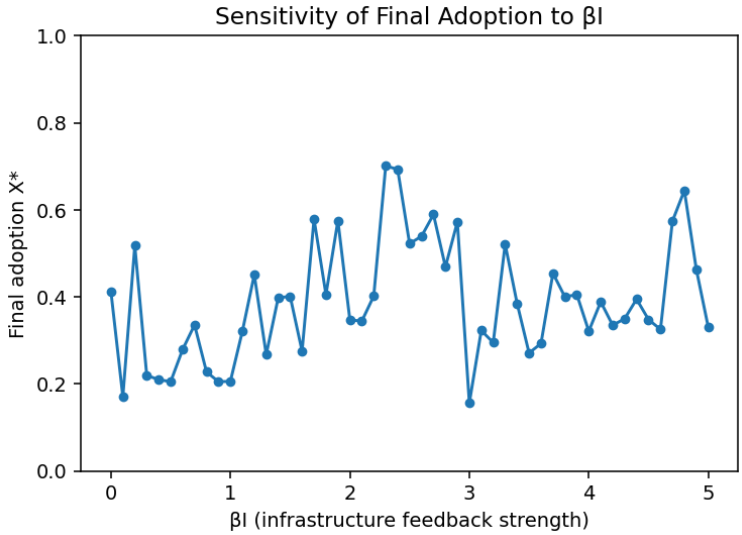

Figure 4: Sensitivity of final adoption X^* to infrastructure feedback strength β_I .

3.2 Network Structure Analysis

Our results show strong interactions between network structure and seeding strategy (Figure 5). Under degree-based seeding, minimal initial adoption ($X_0 \approx 0.05$–0.1) suffices to trigger near-universal diffusion across all topologies. The Barabási–Albert (BA) network reaches full adoption almost immediately, while Erdős–Rényi (ER) and Watts–Strogatz (WS) networks require only slightly higher thresholds. Concentrating early adopters on high-degree nodes increases local coordination incentives; once a hub adopts, the payoffs of its neighbours rise sharply, pushing the network above the critical threshold. Structural barriers thus vanish, rendering topology largely irrelevant when influential agents adopt early. Under random seeding, however, tipping thresholds increase and network-specific effects re-emerge. WS networks transition more easily than ER networks, while BA networks often stall due to delayed hub activation. Without early influential adopters, diffusion remains locally constrained, exposing each topology's structural vulnerabilities.

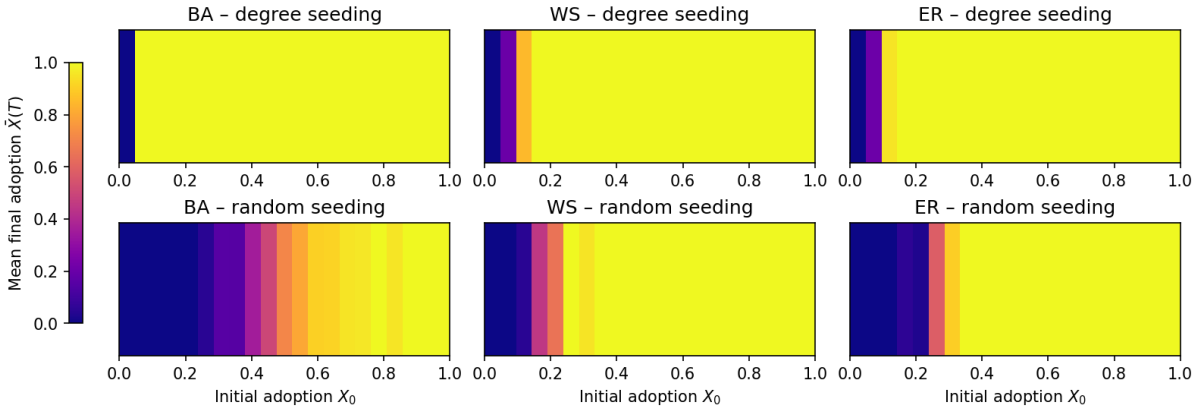

Figure 5: 1-D heatmaps showing mean final adoption as a function of initial adoption X_0, across different network types and seeding strategies.

Mean adoption trajectories (Figure 6) further illustrate how network structure shapes the speed of diffusion for different initial adoption X_0. With degree seeding, all networks converge rapidly, typically within 10–20 steps, likely driven by early hub activation (BA) or dense local reinforcement (WS). In

BA networks, even very small initial adoption leads to fast and complete diffusion, whereas in WS and ER networks adoption may become trapped at lower levels when the tipping threshold is not exceeded.

By contrast, random seeding generates pronounced topological dependence. BA networks exhibit heterogeneous, non-converging trajectories across X_0, with many runs stabilizing at distinct partial-adoption plateaus; for $X_0 < 0.10$, adoption remains at zero. WS networks display partial convergence, with several trajectories aligning at high adoption levels once tipping occurs. ER networks, in contrast, show bimodal outcomes, with trajectories either collapsing to near-zero adoption or accelerating to near-full adoption. Overall, these patterns indicate that network structure primarily governs access to tipping, rather than the speed of diffusion once coordination is achieved.

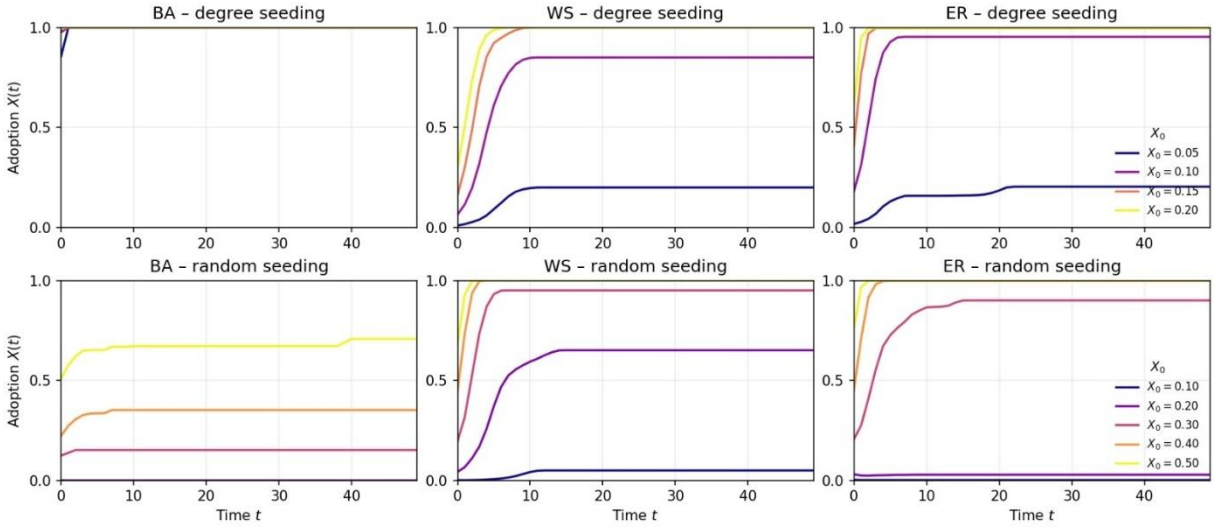

Figure 6: Mean adoption trajectories over time across different network types and seeding strategies.

Figure 7 reports the probability of high adoption ($\geq 80\%$) at tested X_0 values ranging from 0.0 to 1.0 in 0.05 steps. Under degree seeding, BA transitions from $X_0 = 0.05$, while WS and ER both achieve probability 1 by $X_0 = 0.15$, confirming near-certain coordination at very low X_0. Random seeding reveals strong topological contrasts. BA networks remain at zero probability until $X_0 \approx 0.20$, after which the probability increases gradually and irregularly, requiring very high initial adoption to achieve coordination. WS networks exhibit a sharp transition shortly after $X_0 = 0.15$, reaching probability one by $X_0 = 0.25$. ER networks remain at zero until $X_0 = 0.20$, followed by an abrupt jump to full coordination by $X_0 = 0.35$.

The location and steepness of these transitions reflect network-specific sensitivity to tipping. BA networks are most fragile under random diffusion, WS networks are comparatively robust due to local clustering, and ER networks behave as homogeneous systems with a well-defined threshold. Overall, the results demonstrate that targeted seeding largely neutralizes structural constraints, whereas random diffusion exposes the critical dependence of coordination success on network topology.

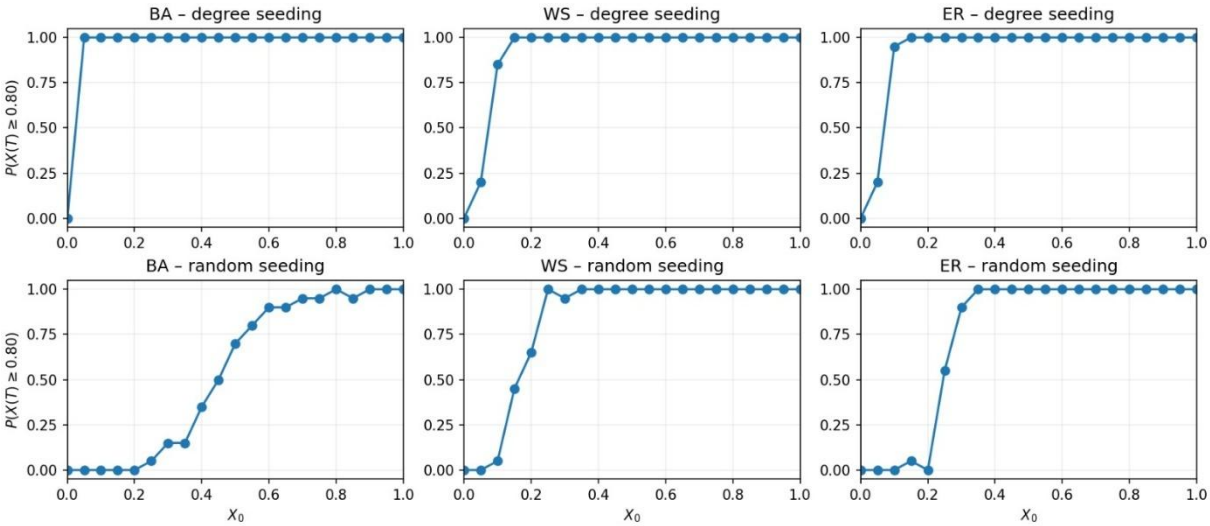

Figure 7: Probability of reaching a high-adoption equilibrium (≥80%) as a function of initial adoption X_0 across network types and seeding strategies. Dots represent tested X_0 values ranging from 0.0 to 1.0 in 0.05 steps.

4. Policy Intervention

4.1 Policy Design

Model results show that EV diffusion is primarily driven by initial adoption, not infrastructure. Early dynamics are dominated by social imitation and highly sensitive to initial conditions. Degree-based seeding outperforms random seeding: targeting highly connected agents reliably triggers diffusion cascades, while untargeted subsidies often fail to overcome coordination barriers. Effective policy design should therefore boost early adoption and target socially central agents.

We propose a targeted, time-limited intervention directed at high-degree social network nodes, implemented through social media influencers. Because baseline EV adoption varies across countries, the intervention supplements existing adopters under country-specific initial conditions. It best fits countries with low EV uptake but high social media engagement, such as several in Eastern Europe.

The intervention distributes free EVs to a fixed share of influencers across diverse sectors, ensuring coverage of multiple social clusters. Influencers promote EV use for one year, during which new adopters are eligible for a temporary purchase subsidy. In model terms, this represents an early, targeted seeding shock among high-degree nodes. The policy rests on two assumptions: (1) influencer reach correlates with network degree, and (2) promotion increases adoption through imitation, matching empirical evidence from influencer marketing. As social media networks follow scale-free (BA) topologies, activating hubs is expected to trigger rapid, self-reinforcing cascades.

4.2 Intervention Results

We compare a no-policy baseline to a targeted policy scenario across ER, WS, and BA networks. The baseline assumes 10% initial EV adoption, while the intervention adds 3% targeted high-degree adopters (influencers). Each scenario averages 40 stochastic runs. While all network types are tested for robustness, BA (scale-free) networks are the most realistic approximation of social media structures.

Across all network types, the targeted intervention substantially outperforms the baseline. In BA networks, adoption increases extremely rapidly and converges to full adoption within the first few time steps (Figure 8). Variability across runs is minimal, as shown by narrow fan-chart bands and

concentrated histograms. Once high adoption is reached, it remains stable even after the subsidy is removed, indicating that the intervention pushes the system beyond a tipping point where diffusion becomes self-sustaining. This highlights the structural fragility of scale-free networks: activating a small fraction of hubs is sufficient to trigger system-wide coordination.

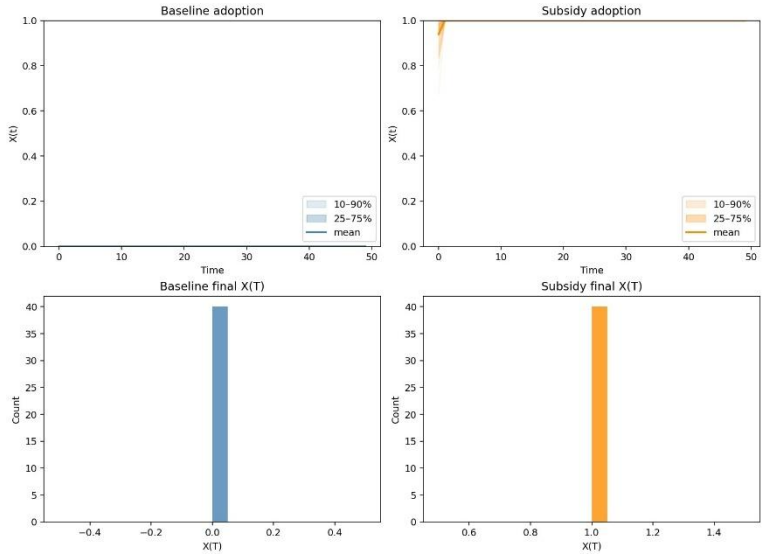

Figure 8: Fan chart and histogram of final EV adoption trajectories in BA (scale-free) networks under baseline and targeted intervention scenarios.

WS networks respond more gradually but still strongly to the intervention (Figure 9). Compared to BA networks, diffusion is slower and slightly more variable, reflecting the role of local clustering. Nevertheless, the policy shifts the adoption distribution decisively toward high-adoption outcomes, with substantially better performance than in the baseline. Some runs remain trapped at low adoption, indicating that clustering can occasionally delay or block full coordination.

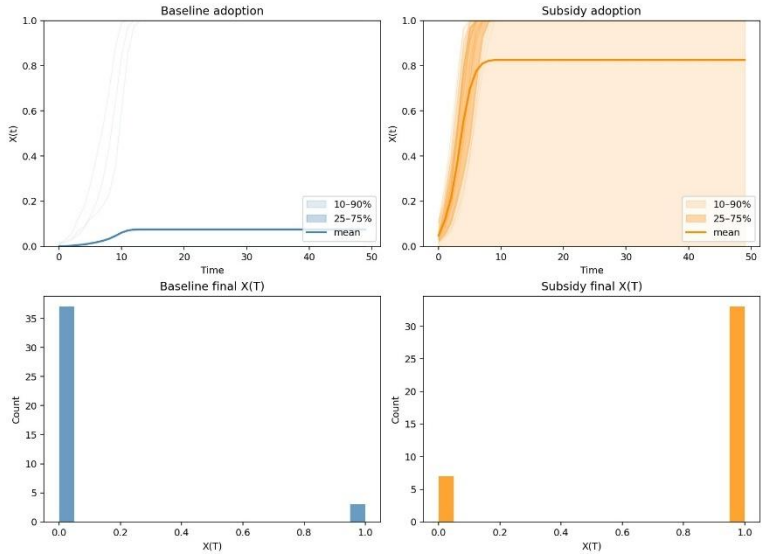

Figure 9: Fan chart and histogram of final EV adoption trajectories in WS (small world) networks under baseline and targeted intervention scenarios.

ER networks are the least responsive (Figure 10). While the intervention increases mean adoption and allows some runs to escape the low-adoption equilibrium, convergence is slower and outcomes are highly variable. The final adoption distribution becomes bimodal, with some runs tipping to high adoption and others remaining near zero. The absence of highly influential hubs limits the effectiveness of targeted seeding, making policy success probabilistic rather than guaranteed.

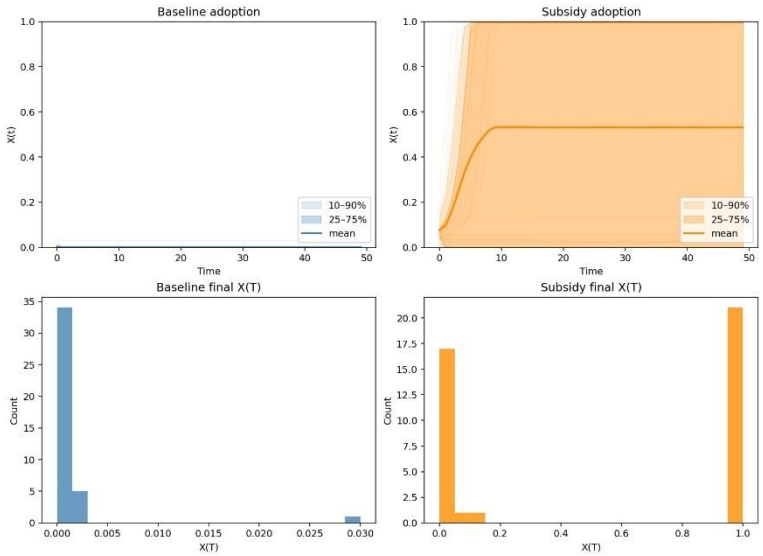

Figure 10: Fan chart and histogram of final EV adoption trajectories in ER (random) networks under baseline and targeted intervention scenarios.

These differences are summarized in Figure 11, which reports the fraction of runs reaching at least 80% adoption. The intervention is almost deterministic in BA networks, typically effective but stochastic in WS networks, and only partially effective in ER networks. The overall effectiveness ranking is BA > WS > ER, which highlights the importance of network structure in overcoming coordination failure.

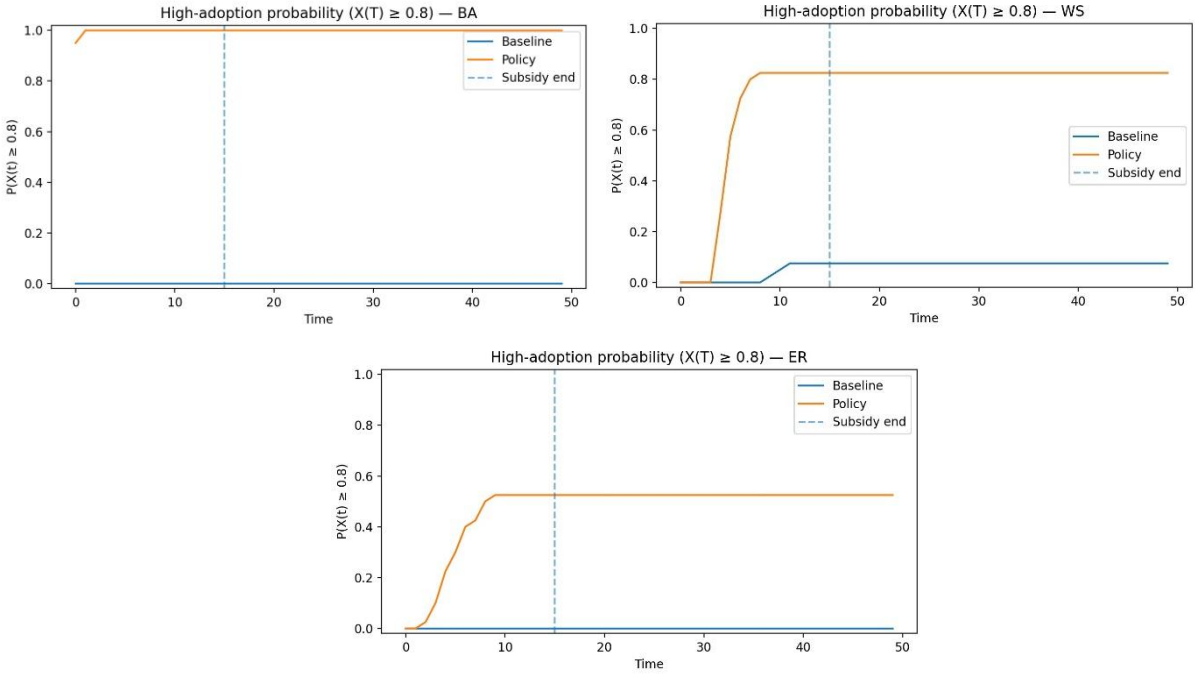

Figure 11: Fraction of simulation runs reaching at least 80% adoption for BA, WS and ER networks.

In a second step, we systematically vary both the fraction of targeted hubs receiving free EVs (1–5%) and the subsidy strength, represented by an increase Δ in the adoption payoff a_0 (Figure 12). In other words, the subsidy raises the attractiveness of EV adoption from a_0 to $a_0 + \Delta$. In BA networks, even very small, targeted giveaways (≈2%) are sufficient to ensure full adoption; subsidy strength plays a secondary role once hubs are activated. WS networks require moderate targeting but remain relatively insensitive to subsidy magnitude. ER networks, by contrast, require simultaneous increases in both targeted seeding and subsidy strength, displaying a broad transition rather than a sharp tipping point. This confirms that in random networks, diffusion relies on cumulative policy pressure rather than structural leverage.

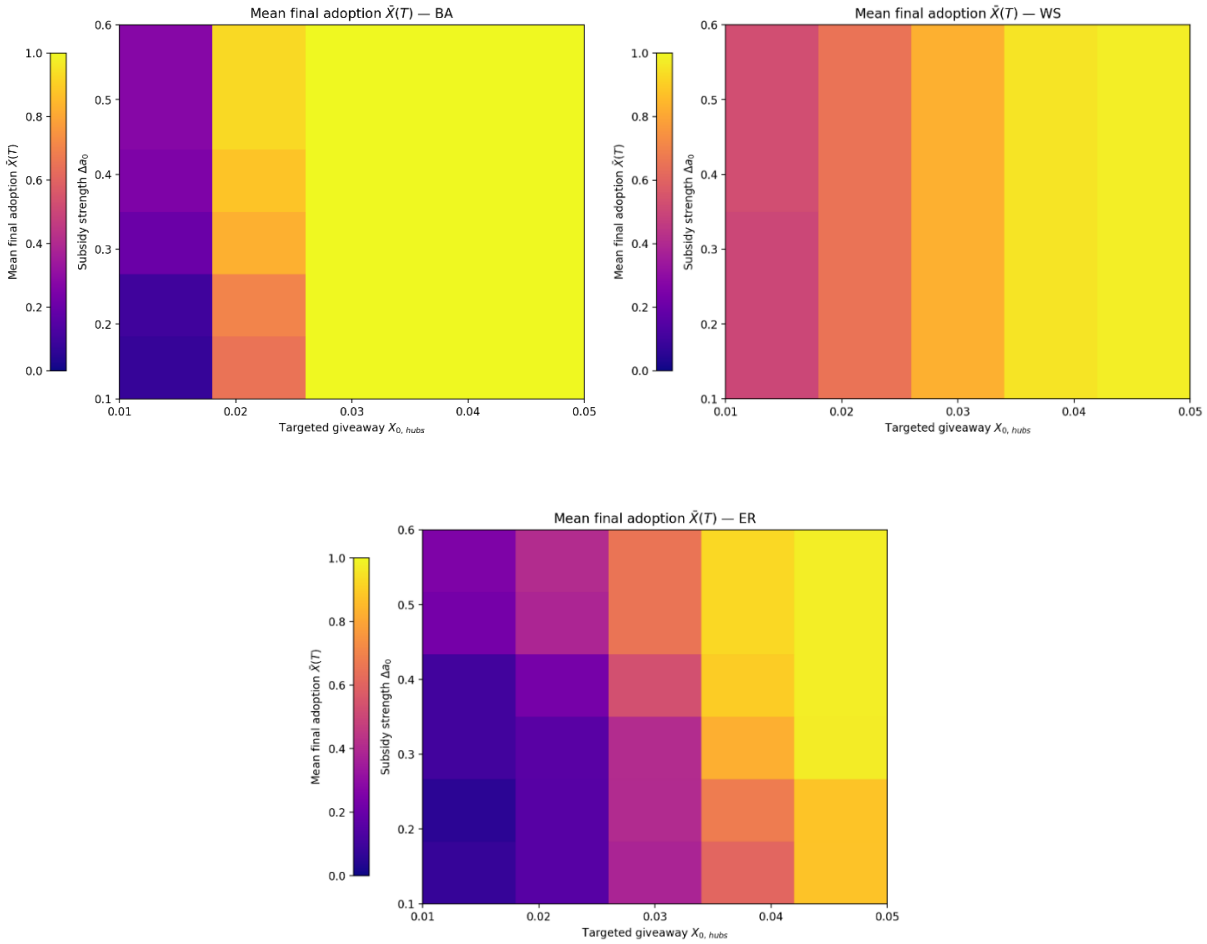

Figure 12: Heatmaps showing the mean final adoption as a function of targeted hub share and subsidy strength.

Finally, varying the duration of the subsidy shows that timing matters primarily in ER networks. In BA and WS networks, adoption converges early and remains stable regardless of when the subsidy ends, indicating that short, early interventions are sufficient once tipping occurs. In ER networks, longer subsidies modestly improve outcomes but do not fully eliminate coordination failure (Figure 13).

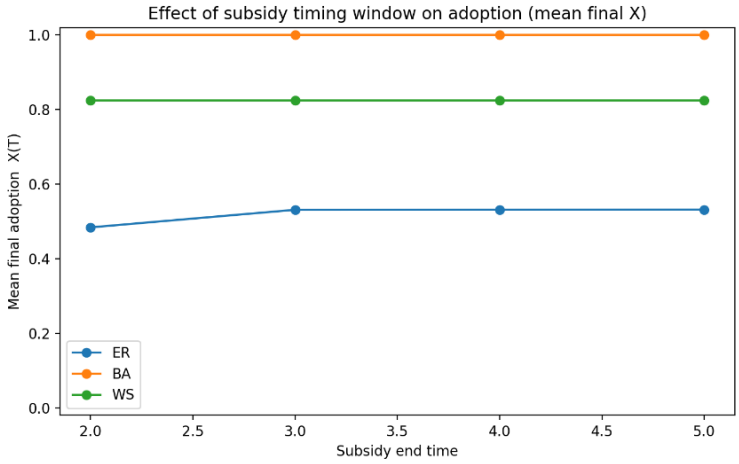

Figure 13: Effect of subsidy duration on final adoption across networks.

Overall, the results show that who is targeted matters more than how many are subsidized. Diffusion depends more on network structure than on subsidy magnitude or duration. Because social media resemble scale-free networks and Eastern European markets combine low EV adoption with high social media engagement, influencer-based targeting can effectively trigger self-sustaining adoption cascades without long-term fiscal support.

4.3. Policy Insight

The proposed intervention is both feasible and scalable. Providing EVs to a limited share of social media influencers entails a fixed and predictable cost, while the one-year duration constrains long-term fiscal exposure. Because influencer marketing is already widely used in private markets, the policy is administratively realistic and likely to face low implementation barriers. From an efficiency perspective, the simulation results suggest that targeting highly connected individuals yields substantially larger diffusion effects than untargeted subsidies, allowing small, upfront investments to trigger large adoption cascades. As such, influencer-based targeted seeding can act as a cost-effective complement to broad purchase subsidies, particularly in countries with low initial EV adoption and highly connected social media environments, where early coordination failures are most pronounced.

5. Limitations & Uncertainty

While the influencer-based intervention is rooted in network analysis and degree targeting, it raises conceptual and ethical issues. For example, providing free electric vehicles to a small, high-visibility group may be perceived as preferential, particularly when done by a democratic government. The policy also assumes that social media is a key information channel, but this may not be the case in all regions or demographics. Its effectiveness is also limited in countries with low social media usage or high levels of existing EV adoption (e.g. Scandinavia), as early adopters are already saturated in these regions.

Furthermore, simulation outcomes are sensitive to network assumptions that consider only ER or scale-free structures. In reality, networks may exhibit clustering, assortativity or temporal dynamics that affect diffusion. The impact of influencers is assumed to be uniform, though real follower responsiveness varies. Stochasticity in adoption and seeding can influence results even when averaging across multiple runs. Parameters such as infrastructure feedback (β_I) and payoff ratios (a_I/b) are stylized representations of complex socio-technical processes. Future work could incorporate heterogeneous agent behaviour, evolving social ties, and empirical influence data to better capture real-world uncertainty.

The adoption process is also stylized. Agents are assumed to respond homogeneously to social influence and incentives, and influencer impact is treated as uniform across agents. In practice, responsiveness varies widely due to differences in preferences, income, and trust, none of which are explicitly represented. Similarly, infrastructure feedback and payoff ratios are modelled using aggregate parameters that approximate complex socio-technical processes, such as charging availability, pricing policies, and perceived convenience. While this abstraction enables exploration of tipping dynamics, it omits fine-grained behavioural and institutional mechanisms.

Finally, the simulations are subject to stochastic variation arising from random network generation, initial seeding, and adoption dynamics. Although outcomes are averaged across multiple realizations to reduce noise, stochasticity remains influential near tipping thresholds, where small perturbations can lead to divergent long-run equilibria. This sensitivity reflects a genuine property of coordination systems but also implies that quantitative results, such as exact tipping locations or adoption probabilities should be interpreted qualitatively rather than as precise forecasts. Future work could mitigate these limitations by incorporating agent heterogeneity, adaptive network structures, and empirically grounded behavioural parameters, thereby improving both realism and predictive power.

6. Reproducibility

All the code used for the experiments, along with instructions regarding how to run it, are publicly available on GitHub.

References

Arthur, W. B. (1989). Competing technologies, increasing returns, and lock-in by historical events. *The Economic Journal, 99*(394), 116–131.

European Commission. (n.d.). *European Climate Law—Climate Action*. European Commission. Retrieved December 9, 2025, from https://climate.ec.europa.eu/eu-action/european-climate-law_en

European Commission. (2021). *Fit for 55 package: Delivering the EU's 2030 climate target on the way to climate neutrality*. European Commission.

European Environment Agency. (2023). *Greenhouse gas emissions from transport in Europe*. EEA.

European Environment Agency. (2024). *Sustainability of Europe's mobility systems* (Report No. 01/2024). Publications Office. https://doi.org/10.2800/8560026

Farmer, J. D., & Foley, D. (2009). The economy needs agent-based modelling. *Nature, 460*(7256), 685–686. https://doi.org/10.1038/460685a

Greenhouse gas emissions from transport in Europe. (2025, November 6). European Environment Agency. https://www.eea.europa.eu/en/analysis/indicators/greenhouse-gas-emissions-from-transport

Holtz, G., Alkemade, F., de Haan, F., Köhler, J., Trutnevyte, E., Luthe, T., Halbe, J., Papachristos, G., Chappin, E., Kwakkel, J., & Ruutu, S. (2015). Prospects of modelling societal transitions: Position paper of an emerging community. *Environmental Innovation and Societal Transitions, 17*, 41–58. https://doi.org/10.1016/j.eist.2015.05.006

Netherlands Enterprise Agency. (2023). *Dutch National Charging Infrastructure Agenda* [Brochure]. https://english.rvo.nl/sites/default/files/2023-07/Brochure%20Dutch%20National%20Charging%20Infrastructure%20Agenda%20online.pdf

Shove, E. (2012). The shadowy side of innovation: Unmaking and sustaining technologies. *Technology Analysis & Strategic Management, 24*(4), 363–375. https://doi.org/10.1080/09537325.2012.662222